proceedings

MDPI

Proceedings

Redox Active Self-Assembled Monolayer Functioning as a pH Actuator †

Divya Balakrishnan [1,2], Wouter Olthuis [2] and César Pascual García [1,*]

[1] Luxembourg Institute of Science and Technology (LIST), 41 Rue du Brill, L-4422 Belvaux, Luxembourg; divya.balakrishnan@list.lu

[2] MESA+ Institute, University of Twente, Drienerlolaan 5, 7522 NB Enschede, The Netherlands; w.olthuis@utwente.nl

* Correspondence: cesar.pascual@list.lu; Tel.: +352-275-888-583

† Presented at the Eurosensors 2018 Conference, Graz, Austria, 9–12 September 2018.

Published: 21 November 2018

Abstract: Using electrochemical control to change the chemical environment in liquids is quite challenging because the small surface to volume ratio offered by traditional cells limits the release or modification of chemicals from the electrodes. Here we present the control of proton concentration (acidity) using a combination of a redox active SAM, which allows ease of fabrication, control of the chemical reactions and repeatability, with a microfluidic design that provides large range and stability over time of the set acidity point, quasi-reversibility during several cycles, and capacity of miniaturization and scalability for multiplexing.

Keywords: microfluidic platform; electrochemical cell; miniaturization; pH control

1. Introduction

Redox active self-assembled monolayers (SAMs) are electrode coatings capable of exchanging electrons and ions with electrolytes facilitating the design of new devices like sensors, batteries, or chemical switches. Novel applications envisioned redox-SAMs with the combination of nanomaterials as external actuators that can change the chemical environment allowing an automatized electrochemical control of parameters like acidity or the concentration of other molecules, however offering a limited impact [1]. We propose that these SAMs combined with microfluidics have the potential of achieving electrochemical control with low actuating voltages to exchange ions with the electrolyte without other side reactions, while providing a larger impact of the surface reactions into the volume liquid due to the control of the microfluidic content.

To this goal we studied Aminothiolphenol SAMs modified by electrochemical, optical and plasma dimerization methods that provided electrode coatings with quasi-reversible redox states able to exchange protons with the electrolyte at low voltages [2]. We correlated their chemical characterization with their electrochemical performance. Due to the short distance of the redox centers with the electrodes, these SAMs exhibited low redox voltages and stabilities during hundreds of cycles necessary for example for applications in combinatorial chemistry. We achieved the control of proton concentration over the liquid with an efficient design of the microfluidic devices to avoid the diffusion of protons and the reduction of hydrogen in the counter electrode, providing long lasting stability of the pH in the cell during several tenths of minutes that can allow the regulation of other chemical reactions [3,4]. The experiments were carried out in an aqueous electrolyte using a pH fluorescence marker to track the pH in the available range and for the more extreme proton concentrations we used calculations based on cyclic voltammetry measurements (CV) to estimate the minimum pH. The protons were confined in nL volumes, which provided the system very large pH

swing. The design we present is compatible with miniaturization and multiplexing, promising devices with a systematic control of acidity.

2. Materials and Methods

2.1. Sample Preparation and Study of Polymerisation Methods of ATP

Silicon substrates with a 50 nm oxide layer were cleaved to obtain 2 × 1 cm^2 samples. The substrates were evaporated with Au 30 nm with an adhesion layer of Ti of 5 nm using an e-beam evaporator. Substrates were then cleaned under a UV ozone lamp for 30 min. 0.5 mM concentration of 4 Aminothiolphenol (4ATP) solution in 30 mL of absolute ethanol was prepared in a beaker. After the completion of UV ozone cleaning, the samples were placed on the thiol solution beaker and covered with aluminum foil. The beaker was placed under a fume hood for overnight functionalization. Three different methods of polymerisation of ATP were performed, Electropolymerisation, Photopolymerisation and Plasmapolymerisation. More details on the setup of the experiments are described in our previous work [2]. The charge transfer for each polymerisation method was measured and compared using CV measurements. The experiments were recorded for the voltage range of −0.2 to 0.7 V at 100 mV/s scan rate.

2.2. Design of the Electrochemical Chip

The electrochemical cell chip was fabricated on a 3 × 3 cm^2 Si Substrate with 50 nm oxide layer using optical lithography. The design consisted of a three electrode electrochemical cell with working (WE), counter (CE) and reference electrodes (RE) separated by diffusion barriers. The electrode material was Au and to increase the surface area the counter and working electrodes were electrochemically platinized. Then all the electrodes were functionalized with 4ATP molecules. The chip was mounted on a microfluidic platform that connects the electrodes to the potentiostat through a switch box. The platform includes an optical window to monitor the pH changes through a fluorescent marker dissolved in the electrolyte. In addition the platform has a pneumatic actuator to open and close the cell. More details about the fabrication methods and the design of the platform were described in our previous work [3,4].

2.3. Electropolymerization and pH Control on the Platform

1 M concentration of potassium chloride solution containing 0.5 μM fluorescence dye carboxy semi-naphthorhodafluors (carboxy SNARFs) was used as the electrolyte. The electropolymerisation was performed with the cell in its open position. The electric signal was controlled with a Solartron Modulab XM Pstat 1 mS/s potentiostat using three electrode configuration. A cyclic voltammogram was programmed in the poteniostat between of −0.9 V to 0.9 V using a scan rate of 50 mV/s for 4 cycles. Before the pH control experiments, the cell was flushed exchanging the electrolyte. The cell was then closed using pneumatic actuator leaving the WE communicate to the RE and CE only through diffusion barriers. A cyclic voltammetry experiment is pre-programmed in the potentiostat for a voltage range of 0.75 V to −0.75 V at a scan rate of 50 mV/s. The fluorescence acquisition was started before the voltage scan, focusing on the signal from the WE.

3. Discussion

Figure 1a(i) shows the structural representation of the self-assembled 4ATP adsorbed on Au, which can dimerize in different ways depending on the polymerisation method (Figure 1a(ii–iv)). We discussed the different possibilities of polymerisation in our previous article [2]. All the three methods provided reversible proton exchange reactions where two protons and two electrons are exchanged from the molecule to the electrolyte. Figure 1b shows representative cyclic voltammograms of the polymerized samples electropolymerized in black, UV polymerized in red and plasma polymerized in blue. All the three methods showed redox active behavior with an oxidation and reduction potential around 0.2 V and 0 V respectively.

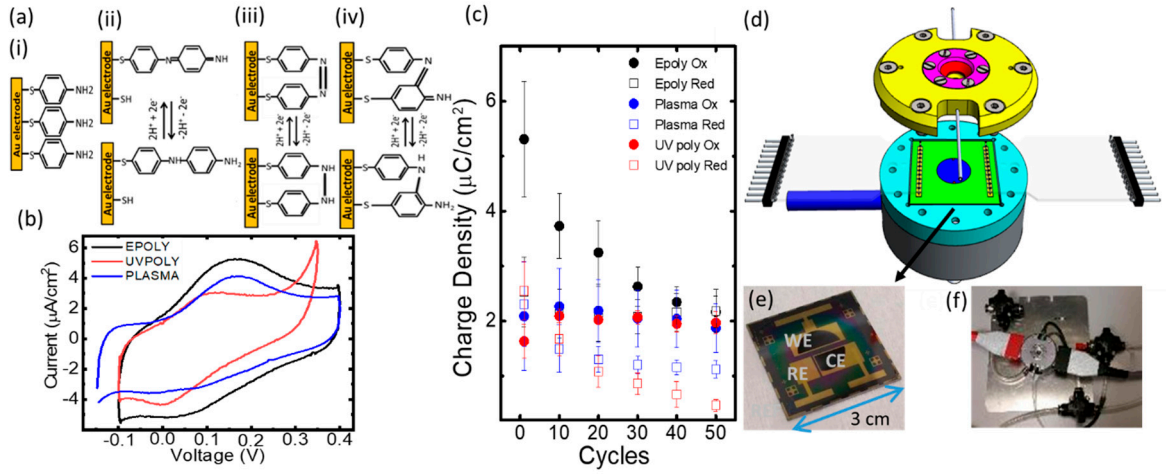

Figure 1. (**a**) Structural representation of (i) Aminothiolphenol, (ii) electropolymerized, (iii–iv) optical and plasma polymerized SAMs on Au electrodes; (**b**) Cyclic voltammograms of the polymerized layers where black, red and blue correspond to electrochemical, optical and plasma methods respectively; (**c**) Charge transfer for oxidation and reduction reactions of 4ATP for different polymerisation methods is plotted against the number of cycles; (**d**) Microfluidic platform suitable for exchangeable chips; (**e**,**f**) Photographic image of the electrochemical chip and the microfluidic platform respectively. (Figure adapted from our previous publication [2,4]).

To study the reversibility of redox reactions of the different polymerisation types the CV measurements were repeated up to 50 cycles. In Figure 1c the charge transfer for the oxidation and reduction peaks are plotted against the number of cycles. We observed that while electropolymerisation initially showed a higher charge transfer respect to the other methods, afterwards, it degraded to approximately the same value of the other polymerisation techniques. On the other hand, the charge transfer of the UV and plasma polymerisation was nearly constant and shows less degradation with successive cycles. The advantage of electropolymerisation is a higher charge transfer at the beginning, however, UV or plasma polymerisations can be more suitable for delivering large batches of samples, and if the application requires many cycles, they do not have much difference of charge transfer after 50 cycles. More details of the characterization and performance of the polymerized layers can be found in our previous work [2].

Figure 1d shows the schematic representation of the microfluidic platform with image of the electrochemical chip in Figure 1e and the platform in Figure 1f. The electrochemical chip was mounted on the microfluidic platform and the working and counter electrodes were electropolymerized by cyclic voltammetry and later flushed with electrolyte for pH control measurements. Figure 2 shows the CV of 8 cycles representing the proton exchange reactions of 4ATP in a closed cell. (a) The applied voltage and (b) the measured current with respect to time are plotted. The corresponding SNARF peak fluorescence from the 650 nm peak (sensitive to proton concentration) was extracted and plotted against time in (c). For each cycle the fluorescence intensity shifts from maximum to minimum and this process is repeated for successive cycles showing reversible pH changes. Using a pH calibration curve of the SNARF fluorescence marker [3] the maximum and minimum intensity exhibited by the SNARF corresponded to pH 7.2 and 5 respectively. However, the minimum pH achieved was beyond the detection range of the SNARF, and using exchange charge from the CV curves and with the volume of the cell, we calculated that the lowest pH was ~0.9 [3].

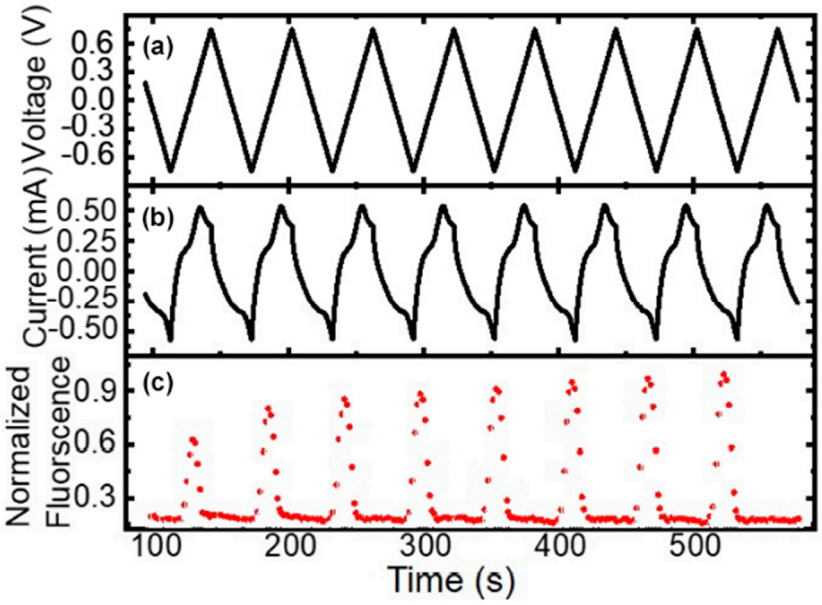

Figure 2. (**a**) Voltage; (**b**) current and (**c**) the intensity of SNARF fluorescence represented as a function of time. (Figure adapted from our previous publication [4]).

In summary, we have reviewed the different types of polymerisation of 4ATP and the efficiency of the redox active reactions. A electrochemical cell was fabricated to function as a pH switch, with the advantages of a miniaturizable design (in the nL range), a large pH range (from neutral to below 1), long lasting stability of the pH contrast between cells over time (tens of minutes), and repeatability during hundreds of cycles.

Author Contributions: D.B. contributed on the performance and design of experiments, writing of the manuscript and preparation of the figures. W.O. contributed to the design and interpretation of the experiments. C.P.-G. provided the original idea of the study, contributed in all the steps of the design and performance of the experiments and the preparation of the article.

Acknowledgments: This work was funded by FNR ATTRACT project 5718158 NANOpH.

Conflicts of Interest: The authors declare no conflict of interest.

References

1. Penner, R.M. Electrochemistry on tap. *Nat. Chem.* **2010**, *2*, 251–252.
2. Balakrishnan, D.; Lamblin, G.; Thomann, J.S.; Guillot, J.; Duday, D.; van den Berg, A.; Olthuis, W.; Pascual Garcia, C. Influence of polymerisation on the reversibility of low-energy proton exchange reactions by Para-Aminothiolphenol. *Sci. Rep.* **2017**, *7*, 15401, doi:10.1038/s41598-017-13589-5.
3. Balakrishnan, D.; Lamblin, G.; Thomann, J.S.; van den Berg, A.; Olthuis, W.; Pascual Garcia, C. Electrochemical control of pH in nano-litre volumes. *Nano Lett.* **2018**, *18*, 2807–2815, doi:10.1021/acs.nanolett.7b05054.
4. Balakrishnan, D.; Gerard, M.; Girod, S.; Frari, D.D.; Olthuis, W.; Pascual Garcia, C. Redox active polymer a pH actuator on a Re-sealable microfluidic platform. *J. Mater. Sci. Eng.* **2018**, *7*, 456, doi:10.4172/2169-0022.1000456.